Electronic Supplementary Material for

The composition and growth mechanism of coexisting $4M_2$ and $4A_8$ biotite polytypes from rhyolite of Long Valley Caldera, California

Jiaxin Xi[a,b,c], Yiping Yang[a,b], Lingya Ma[a,b,c*], Hongping He[a,b,c], Huifang Xu[d], Jianxi Zhu[a,b,c], Jingming Wei[a,b,c]

[a] *CAS Key Laboratory of Mineralogy and Metallogeny / Guangdong Provincial Key Laboratory of Mineral Physics and Materials, Guangzhou Institute of Geochemistry, Chinese Academy of Sciences, Guangzhou 510640, China*

[b] *CAS Center for Excellence in Deep Earth Science, Guangzhou, 510640, China*

[c] *University of Chinese Academy of Sciences, Beijing 100049, China*

[d] *Department of Geoscience, University of Wisconsin-Madison, 1215 West Dayton Street, Madison, Wisconsin 53706, U.S.A.*

*Correspondence to: L.Y. Ma (malingya@gig.ac.cn)

This PDF file includes:

Tables S1 and S2

Figures S1 to S5

Table S1 *k*-factors for annite observed via TEM (FEI Talos F200S)[a, b, c]

Standard	Element Ratio	*k*-factor ($k_{x\text{-}Si}$)
Standard 1*M* biotite	Na/Si	0.41
	K/Si	0.97
	Mg/Si	0.75
	Fe/Si	1.28
	Al/Si	0.69
	Ti/Si	1.10
	Mn/Si	1.14

[a] Conditions: X tilt = 0°, Y tilt = 0°, spot size = 5.
[b] *k* is a sensitivity factor that relates elemental peak intensity to concentration: $C_A/C_B = k_{AB} \times I_A/I_B$.
[c] The *k* for each element was determined based on the content data of 1*M*, $4M_2$, and $4A_8$ biotite.

Table S2 The estimated standard deviations (ESD) of 1*M*, 4A_8-, and 4M_2- annite samples

Element Polytype	1*M*	4A_8	4M_2	Average value
Fe	0.053	0.051	0.056	0.053
K	0.024	0.049	0.029	0.037
Si	0.043	0.038	0.050	0.044
Mg	0.027	0.031	0.030	0.030

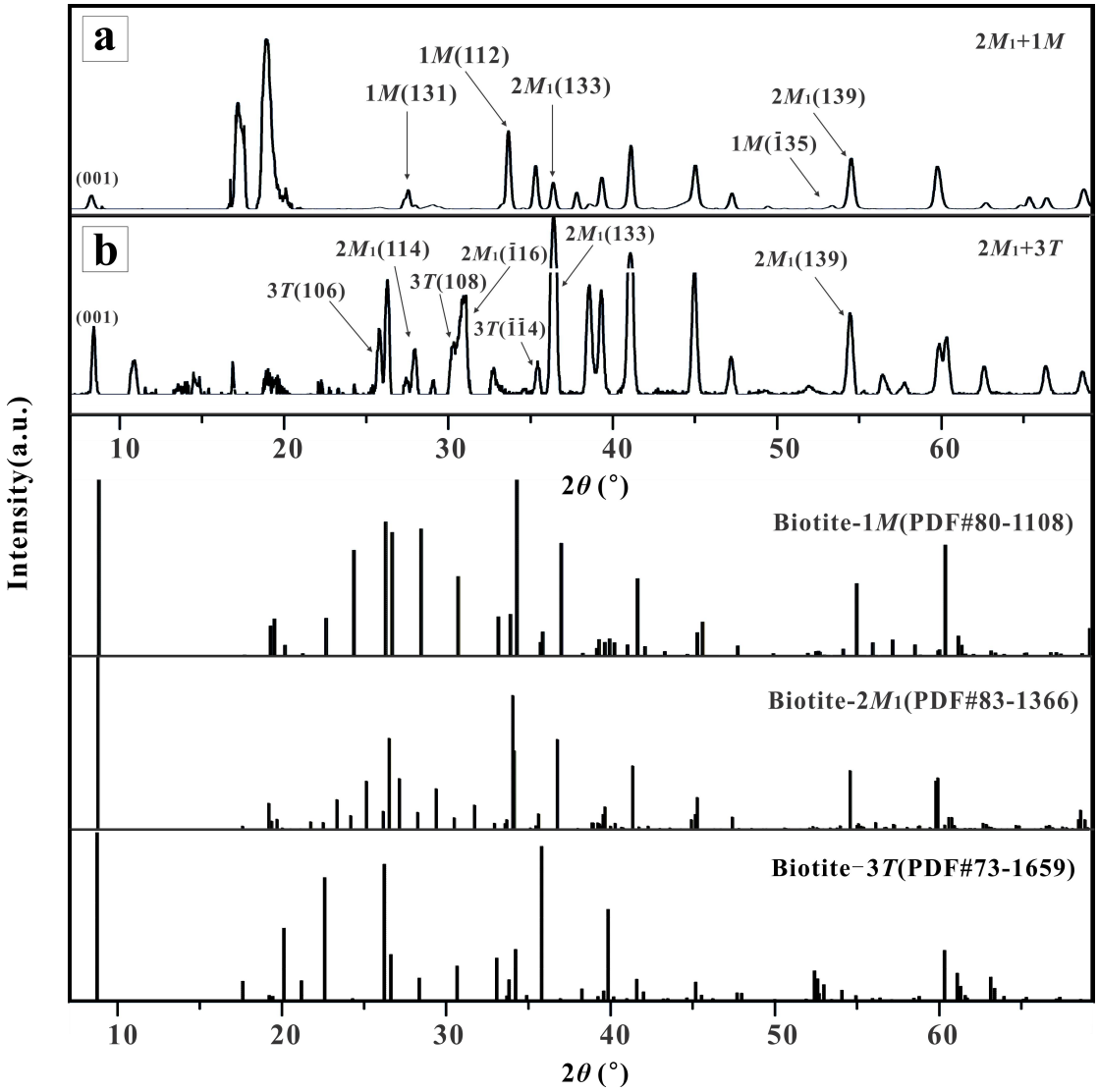

Fig. S1 Complete micro-X-ray diffraction (μ-XRD) patterns of biotite samples (Fig. 1a) and standard 1*M,* 2M_1, and 3*T* biotite PDF cards. (a) corresponds to the upper diffraction pattern of Fig. 1a in the text, and (b) corresponds to the lower diffraction pattern of Fig. 1a in the text.

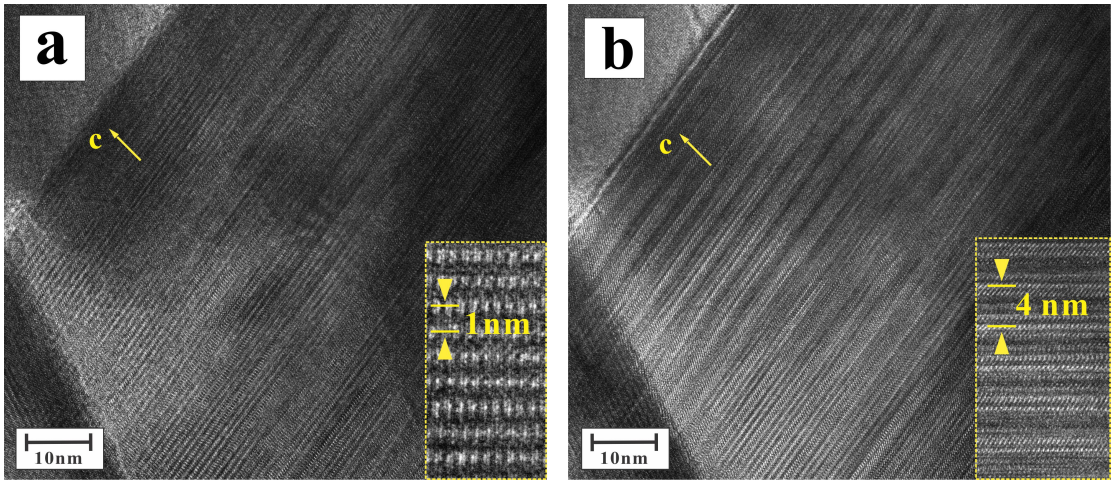

Fig. S2 HRTEM images of one 4-layer biotite: (a) HRTEM image from [110] zone axis showing a periodic repetition of 1 nm (right-bottom inset). (b) One-dimensional lattice fringe image with the crystal slightly tilted (~3°) about the *c*-axis from (a); the image shows a periodic repetition of 4 nm (right-bottom inset).

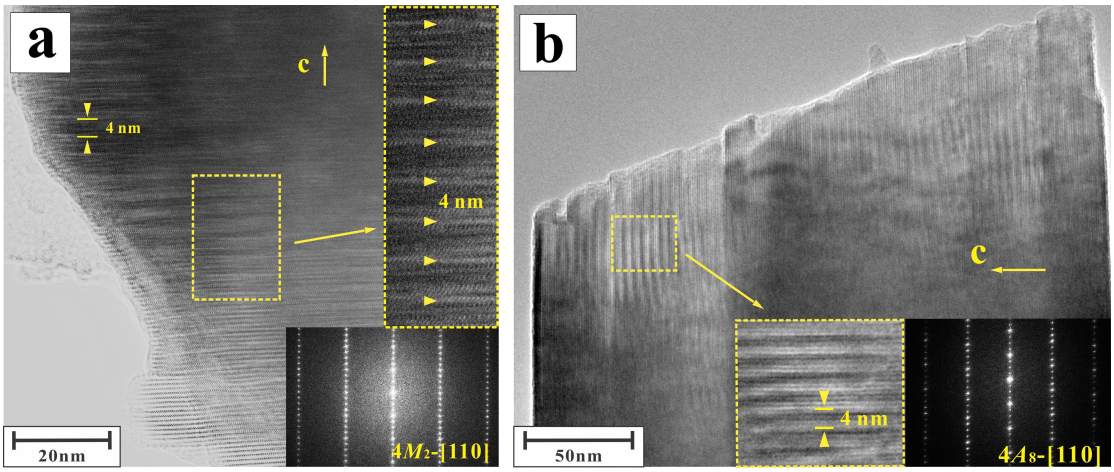

Fig. S3 One-dimensional HRTEM images of representative four-layer biotite domains (with FFT patterns inserted at the right bottom of both images), as the supplement to Figs. 3(a–b) in the text; the images also show the periodic shift after every four layers. (a) $4M_2$ biotite domain, the same as Fig. 3(a) in the text; (b) $4A_8$ biotite domain, the same as Fig. 3b in the text.

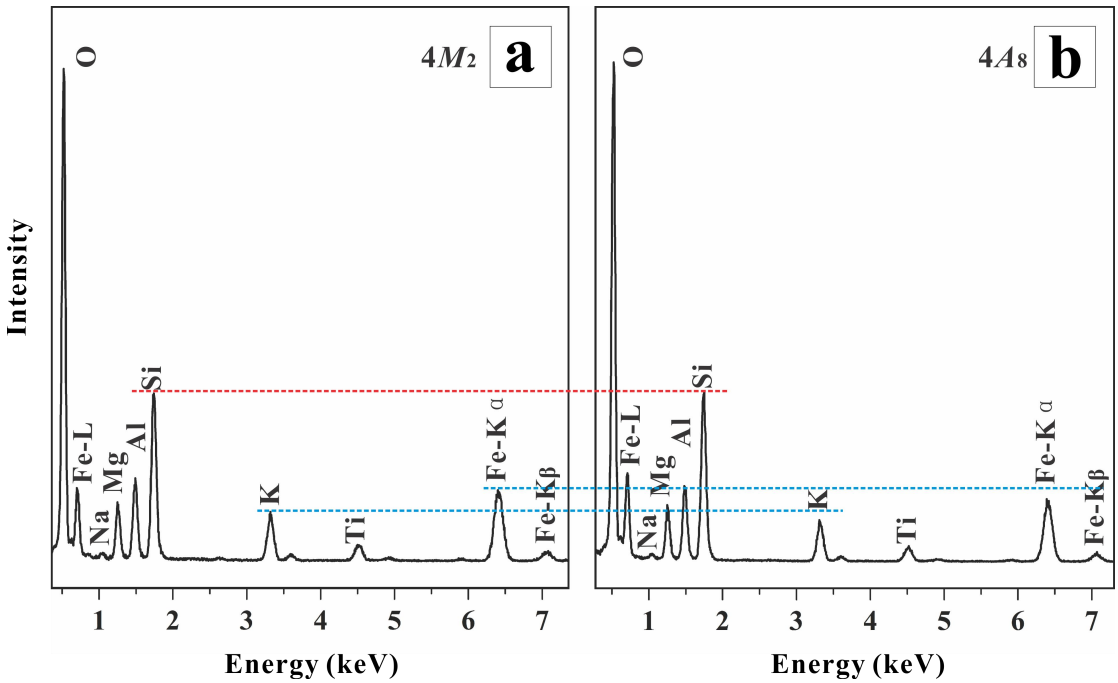

Fig. S4 Energy-dispersive X-ray spectroscopy (EDS) spectrum of two 4-layer polytypes of biotite. To compare the relative spectral height of cations, the intensities of Si in (a) $4M_2$ biotite domains and (b) $4A_8$ biotite domains have been normalized to the same mathematical heights.

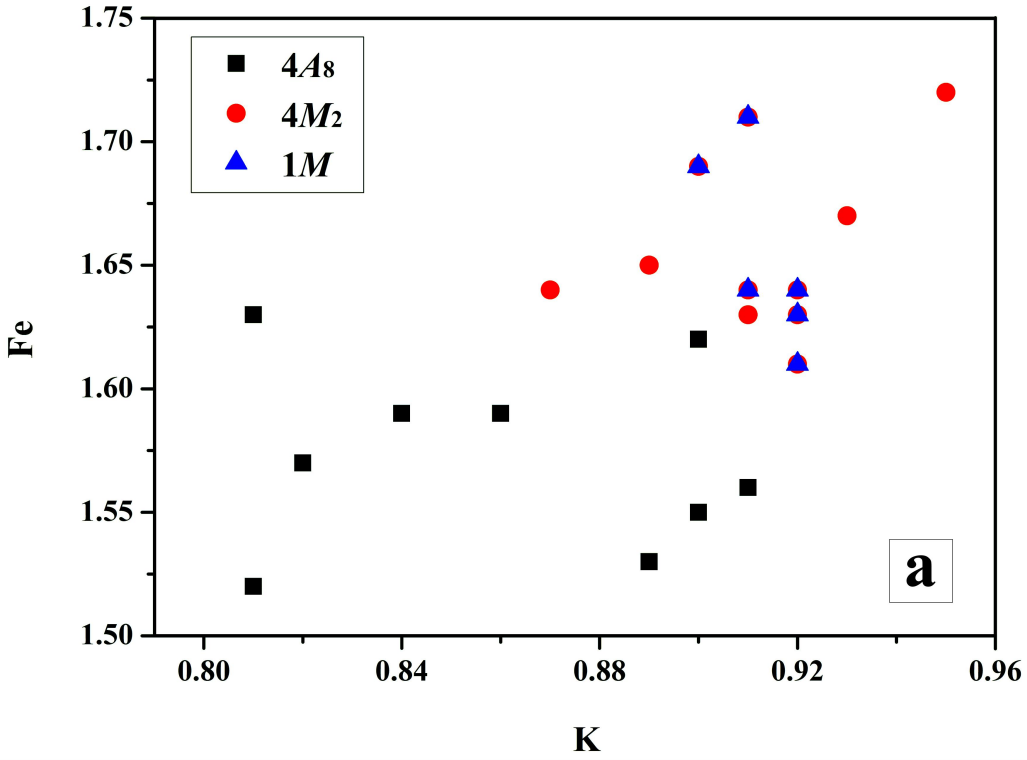

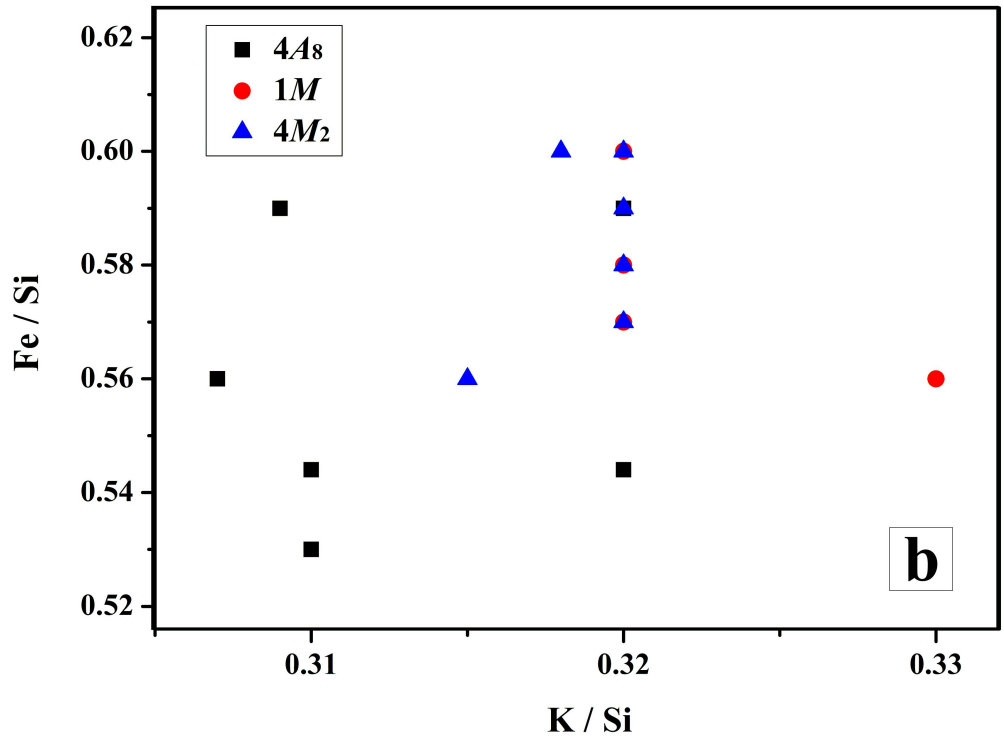

Fig. S5 Diagrams showing the relationship between the (a) K/Fe ratio and (b) K/Si and Fe/Si ratios of 1*M*, 4A_8, and 4M_2 biotite domains.